Molecules and Cells

# Iron Homeostasis Controls Myeloid Blood Cell Differentiation in *Drosophila*

Sunggyu Yoon[1], Bumsik Cho[1], Mingyu Shin[1], Ferdinand Koranteng[1], Nuri Cha[1], and Jiwon Shim[1,2,3,*]

[1]Department of Life Sciences, College of Natural Science, Hanyang University, Seoul 04763, Korea, [2]Research Institute for Convergence of Basic Sciences, Hanyang University, Seoul 04763, Korea, [3]Research Institute for Natural Science, Hanyang University, Seoul 04763, Korea
*Correspondence: jshim@hanyang.ac.kr
http://dx.doi.org/10.14348/molcells.2017.0287
www.molcells.org

Iron is an essential divalent ion for aerobic life. Life has evolved to maintain iron homeostasis for normal cellular and physiological functions and therefore imbalances in iron levels exert a wide range of consequences. Responses to iron dysregulation in blood development, however, remain elusive. Here, we found that iron homeostasis is critical for differentiation of *Drosophila* blood cells in the larval hematopoietic organ, called the lymph gland. Supplementation of an iron chelator, bathophenanthroline disulfate (BPS) results in an excessive differentiation of the crystal cell in the lymph gland. This phenotype is recapitulated by loss of *Fer1HCH* in the intestine, indicating that reduced levels of systemic iron enhances crystal cell differentiation. Detailed analysis of *Fer1HCH-tagged-GFP* revealed that *Fer1HCH* is also expressed in the hematopoietic systems. Lastly, blocking *Fer1HCH* expression in the mature blood cells showed marked increase in the blood differentiation of both crystal cells and plasmatocytes. Thus, our work suggests a relevance of systemic and local iron homeostasis in blood differentiation, prompting further investigation of molecular mechanisms underlying iron regulation and cell fate determination in the hematopoietic system.

**Keywords:** blood, BPS, crystal cell, *Drosophila*, ferritin, Fer1HCH, FAC, hemocyte, intestine, iron, lymph gland, plasmatocyte

## INTRODUCTION

*Drosophila* expresses blood cells that are most akin to the myeloid blood in vertebrates and has been a useful animal model system for hematopoiesis (Gold and Bruckner, 2015; Letourneau et al., 2016; Shim, 2015; Waltzer et al., 2010). Hematopoiesis of *Drosophila* takes place in two distinct phases: first in the embryonic head mesoderm and later in the larval lymph gland. Blood cells originating from the embryonic head become blood cells which travel the embryo. These cells later form the circulating and sessile blood population that collectively function in innate immune responses during larval stages (Evans et al., 2003). In *Drosophila*, there are at least three terminally differentiated mature blood cell types: plasmatocytes, crystal cells and lamellocytes (Jung et al., 2005). The plasmatocyte functions similar to macrophages and constitutes around 95% of total blood cells. Hemolectin (Hml) and Peroxidasin (Pxn) are plasmatocyte markers which are useful in *Drosophila* blood analysis (Jung et al., 2005). The crystal cell is a non-phagocytic cell that plays a role in melanization and wound healing, constituting about 5% of total blood population. Notch is essential for the crystal cell development together with a Runx family transcription factor, Lozenge (Lz) (Lebestky et al., 2003; Mukherjee et al., 2011). The last cell type, the lamellocyte, is

Received 6 November, 2017; accepted 12 November, 2017; published online 14 December, 2017

eISSN: 0219-1032

a rare cell type that is produced upon immune challenges and participates in encapsulation (Lanot et al., 2001; Rizki and Rizki, 1978; Rizki et al., 1985; Sorrentino et al., 2002). Differentiation of lamellocytes requires activation of Toll, JAK/STAT or JNK pathways, a signaling component triggered by stress responses (Agaisse and Perrimon, 2004; Qiu et al., 1998; Zettervall et al., 2004).

The second wave of hematopoiesis occurs in a specialized organ, called the lymph gland, where blood progenitors proliferate and differentiate into mature blood cells. The lymph gland is composed of three zones: the posterior signaling center (PSC), the medullary zone (MZ) and the cortical zone (CZ) (Fig. 1A). The MZ is located at the inner core of the lymph gland and harbors undifferentiated progenitor

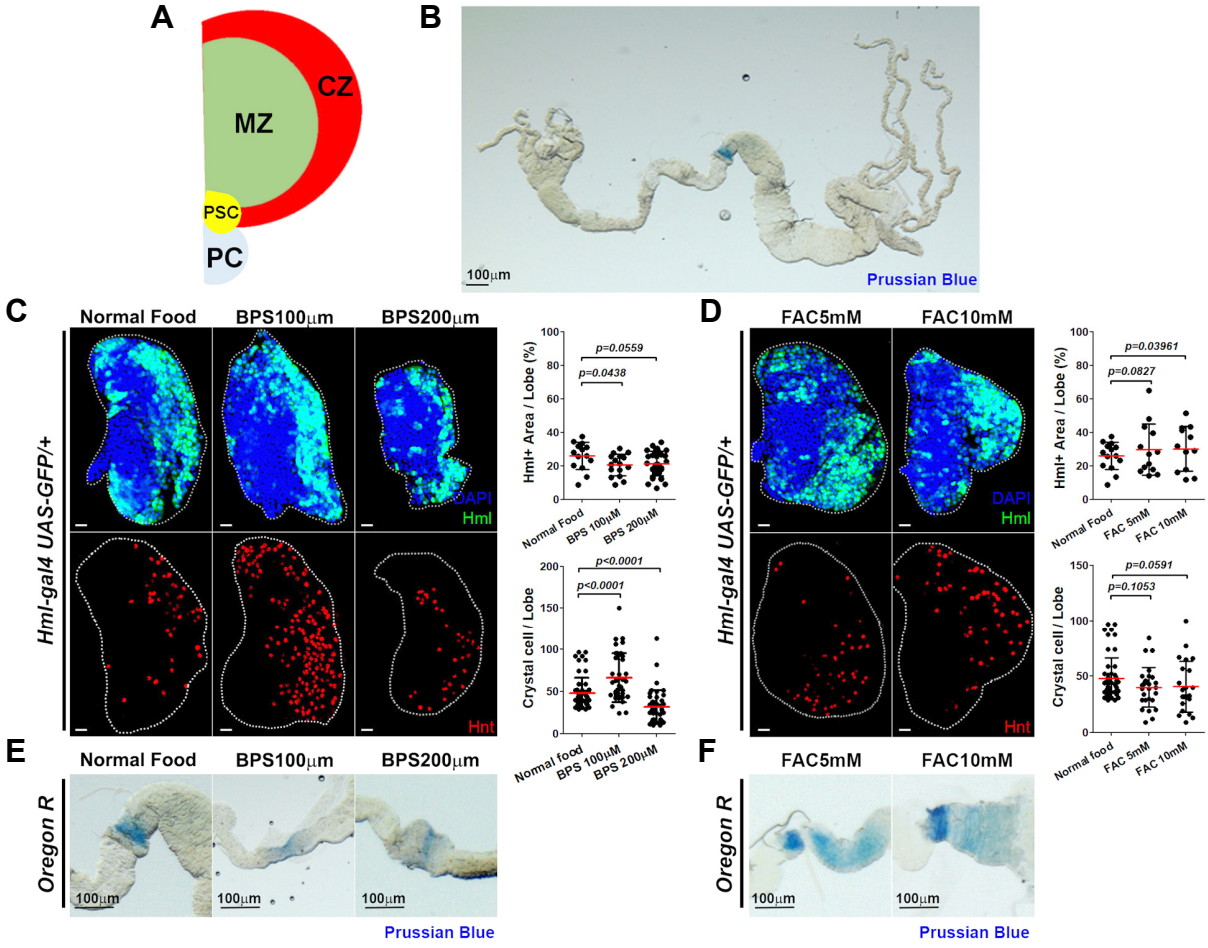


**Fig. 1. Inhibition of iron uptake induces crystal cell differentiation.** (A) Schematic diagram of the lymph gland. PC; pericardial cells, PSC; posterior signaling center, MZ; Medullary zone, CZ; Cortical zone. (B) Expression of Prussian blue in the entire larval gut. Prussian blue displays blue color on reacting with ferric ions. Blue color is specifically observed in the midgut iron region when animals are reared upon regular cornmeal-dextrose media. (C) Iron chelation activates differentiation of crystal cells in the lymph gland. (Top) Hml-GFP indicates expression of mature blood cells which on average is 30% of one lymph gland lobe. This expression is unchanged after feeding 100 μM or 200 μM BPS. 200 μM BPS reduces the size of the lymph gland (Hml, green; DAPI, blue). Quantitation of Hml+ area per lymph gland lobe is indicated in the graph. (Bottom) Expression of crystal cells in the lymph gland is upregulated when animals are reared upon fly media containing 100 μM BPS. 200 μM BPS leads to decreased number of crystal cells associated with small size of the lymph glands (Hnt, red). Quantitation of Hnt+ crystal cells per lymph gland lobe is indicated in the graph. (D) Feeding additional iron does not affect blood development. (Top) Ratios of Hml+ mature blood cells are not altered by feeding either 5 mM or 10 mM FAC (Hml, green; DAPI, blue). Quantitation of Hml+ area per lymph gland lobe is shown in the graph. (Bottom) The number of crystal cells upon excessive iron feeding is not changed (Hnt, red). Quantitation of Hnt+ crystal cells per lymph gland lobe is shown in the graph. (E) Supplementation of BPS reduces the level of iron in the midgut. Prussian blue staining is diminished by feeding 100 μM BPS or 200 μM BPS when compared to larvae cultured on normal food (Prussian blue, blue). (F) Feeding additional iron in the form of FAC accumulates iron levels in the midgut. Iron region expresses Prussian blue in a wider range at higher levels when animals are reared on food containing 5 mM FAC or 10 mM FAC (Prussian blue, blue). Lymph glands are demarcated by white dotted lines. *p* values are indicated in the graphs. Error bars in the graph represent standard deviation. Scale bar, 20 μm unless otherwise indicated.

blood cells. Domeless (Dome) is a JAK/STAT receptor and a hallmark of the progenitor cells diminished during differentiation (Morin-Poulard et al., 2013). Progenitors in the MZ give rise to mature blood cells that comprise the CZ at the periphery of lymph gland. The PSC is a signaling center for the control of MZ and CZ, and also known to control immune responses (Khadilkar et al., 2017; Mandal et al., 2007; Sinenko et al., 2011). Under normal growing conditions, blood progenitors in the MZ develop into either plasmatocytes or crystal cells at constant rates and do not leave the lymph gland until pupariation (Grigorian et al., 2011). However, upon parasitization or stress conditions, progenitors aberrantly change their fate and precociously differentiate into mature blood cells (Sorrentino et al., 2002). In addition, normal ratios of plasmatocytes, crystal cells and lamellocytes are disrupted by stress signals impinging on pathways involved in cell fate determination of the blood. Both local and systemic factors modify blood cell development during stress responses. *Drosophila* genetics allows precise investigations into direct genetic interactions of several local or systemic factors linking blood differentiation and stress response. Hypoxia accelerates differentiation of crystal cells by stabilizing Notch through Hif1α (Sima in *Drosophila*) (Mukherjee et al., 2011). Excessive reactive oxygen species (ROS) leads to precocious differentiation of blood progenitors into mature blood cells (Owusu-Ansah and Banerjee, 2009). Nutrition maintains blood progenitors through the systemic insulin Dilp2 (Benmimoun et al., 2012; Dragojlovic-Munther and Martinez-Agosto, 2012; Shim et al., 2012). Olfactory sensory cue is also important for blood progenitor maintenance through the systemic factor, GABA (Shim et al., 2013). Given that myeloid blood cells are sentinels for stress reactions, further investigation is necessary for unraveling novel molecular mechanisms underlying systemic stress responses of blood cells.

Iron is one of the most abundant transition metal on earth and is an essential element of life. Iron is commonly found in heme-containing enzymes or in iron-sulfur clusters, or as mono- or di-nuclear irons (Ponka, 1997; Rouault and Tong, 2005; Sheftel et al., 2012). Since iron is highly reactive to oxygen, iron has become a key element in aerobic life through evolution. Intracellular and extracellular iron levels are tightly regulated to ensure availability and protection from cellular damages due to high iron concentration (De Domenico et al., 2008). In *Drosophila*, iron is acquired from diet and its absorption takes place at a specific region of the intestine called the iron region (Fig. 1B). Molecular components involved in iron absorption, storage and allocation are conserved in *Drosophila* and known to respond well to changes in iron levels (Mandilaras et al., 2013). Ferritin comprises a heteropolymeric complex that is composed of 12 Heavy (H) and 12 Light (L) chain subunits where iron molecules are stored as a primary storage site (Santambrogio et al., 1996). Expression of ferritin genes are controlled during translation by iron regulatory protein (IRP) that binds to an iron responsive element (IRE) at the 5' UTR of ferritin mRNAs (Georgieva et al., 1999). *Drosophila* genome encodes three ferritin genes: *Ferritin 1 heavy chain* homolog (*Fer1HCH*), *Ferritin 2 light chain* homolog (*Fer2LCH*) and *Ferritin 3 heavy chain* homolog (*Fer3HCH*). Fer1HCH and Fer2LCH together generate the major ferritin complex while Fer3HCH belongs to the mitochondrial ferritin family abundant in testes (Mandilaras et al., 2013; Missirlis et al., 2006). Loss of *Fer1HCH* or *Fer2LCH* results in a wide range of developmental defects in multiple tissues associated with cuticle deposition, dorsal closure, head involution and nervous system development in embryo (Gonzalez-Morales et al., 2015). In larvae, expression of RNAi against *Fer1HCH* or *Fer2LCH* in the intestine leads to growth retardation from early instars. In addition, eye-specific RNAi of ferritin genes causes an abnormal compound eye phenotype, and with neuron-specific drivers, neurodegenerative vacuoles are generated due to high levels of iron (Tang and Zhou, 2013). Sequestration of iron during innate immune responses is critical for mounting immune reactions and is evolutionarily conserved from *Drosophila* to mammals (Drakesmith and Prentice, 2012). However, it is unclear whether iron levels are associated with blood cell development or whether blood cells actively participate in iron homeostasis by expressing iron regulators or both.

In this study, we used genetic approaches to decipher possible roles for iron homeostasis in *Drosophila* blood cell development. Disrupting iron homeostasis by supplementing iron chelator BPS or loss of *Fer1HCH* in the intestine causes excessive differentiation of crystal cells in the lymph gland. We discovered that blood cells also express *Fer1HCH* in addition to the previously identified organs. Correlated to these findings, loss of *Fer1HCH* in mature blood cells is sufficient to induce crystal cell as well as plasmatocyte differentiation. Thus, this work establishes iron homeostasis as a crucial factor in *Drosophila* blood development and this key role is modulated by ferritin which is expressed significantly in the blood or in the intestine.

## MATERIALS AND METHODS

### Fly stocks and genetics

The following fly stock lines were used in this study: Oregon R, NP1-gal4 (DGRC112001), $Mvl^{NP2375}$-gal4 (DGRC104178), Hml-gal4 (S. Sinenko), Pxn-gal4 (J. Fessler), Dome-Meso-gal4 (U. Banerjee), nSyb-gal4 (BL51635), $Hml^{LT}$-gal4 (U. Banerjee), Ppl-gal4 (BL58768), UAS-Hid,Rpr (Nambu JR), $Fer1HCH^{RNAi}$ (BL60000), $Fer2LCH^{RNAi}$ (BL44067), $IRP\text{-}1A^{RNAi}$ (BL58117), $IRP\text{-}1B^{RNAi}$ (BL61246), $mfrn^{RNAi}$ (BL34038), $mvl^{RNAi}$ (BL55316), $Tsf1^{RNAi}$ (BL55936), $Tsf3^{RNAi}$ (BL56015) and $Fer1HCH^{G188}$ (DGRC110620). Crosses were kept at 25℃ for efficient mating and moved to 29℃ to maximize expressions. FAC/BPS feeding experiments were done at 25℃.

### Circulating blood cell RT-qPCR

RNA from blood cells were extracted from 30 third instar larvae. First strand cDNA was synthesized using ReverTra ACE® qPCR RT Kit (Toyobo). Relative quantitative PCR was performed by comparative $C_T$ method using SYBR Green® Realtime PCR Master Mix (Toyobo) and StepOne Real-time PCR detection thermal cycler (Applied Biosystems). Two sets of primers were used to detect *Fer1HCH* mRNA. Primer set 1: 5'-CTGCTCCTGTTGGCCGTGGT-3' (Forward) and 5'-TCCTTCATGTCCACCCAGTCCT-3' (Reverse). Primer set 2: 5'-ATGGT

GAAACTAATTGCTAGC-3' (Forward) and 5'-TCAGATCGCTG ACTCCCTC-3' (Reverse). Levels of *RpL32* were used to normalize total cDNA.

### Prussian blue staining

Guts from wandering third instar larvae were dissected in PBS, transferred to 3.7% formaldehyde/PBS and fixed for 30 min. Samples were then treated with 1% Tween20 in PBS for 15 min. To detect the ferric iron in the gut, tissues were stained with freshly-made Prussian blue staining solution (2% HCl and 3% potassium hexacyanoferrate (II) trihydrate; Sigma P3289) for 45 min in dark condition. After staining, samples were washed in PBS 3 times for 2 min each. Lastly, guts were mounted in VECTASHIELD® solution and imaging was done with Nikon microscope SMZ18.

### FAC, BPS feeding

Parent flies were raised and crossed in standard medium. 3 days later, crossed flies were transferred into conditioned medium supplemented with 5 mM FAC (Ferric Ammonium Citrate; Sigma F5879), 10 mM FAC, 100 μM BPS (Bathophenanthrolinedisulfonic acid disodium salt; Sigma B1375) or 200 μM BPS. Eggs were reared in iron-supplemented or iron-chelated medium at 25℃ and wandering third instar larvae were dissected.

### Immunohistochemistry

Wandering third instar larvae were dissected in 1X PBS solution at room temperature. All collected organs were fixed in 3.7% paraformaldehyde for 30 min at room temperature. Washing was done in 0.4% 1X PBS TritonX100 for 10 min and repeated 3 times. Samples were blocked in 10% NGS for 30 min and then treated with primary antibody overnight at 4℃. After another wash, samples were treated with secondary antibody for 3 h. Samples were washed again as described earlier and rewashed in 1x PBS before kept in VECTASHIELD® (with DAPI). The following primary antibodies were used in this study: Rabbit αPxn (1:2000), Mouse αHnt (1:10 DSHB), Rabbit αcleaved Caspase3 (1:300 Cell signaling #9661) and Rabbit αRab5 (1:1000 AbCam #ab31261). The secondary antibodies used are: FITC or Cy3 conjugated antibodies using a 1:250 dilution (Jackson ImmunoResearch Laboratories).

To generate antisera specific for the Pxn protein, a peptide corresponding to amino acids 326-342 of Pxn sequence (NGGNHPLDSPIDARSNQ) was used as antigen in rabbits (Ab Frontier, Korea).

### Quantification of the lymph gland phenotype

Lymph gland staining was quantified as previously described (Shim et al., 2012). In brief: for Hml, Pxn or Dome images, middle one third stacks were compressed and analyzed using ImageJ. For Hnt-positive cells, 3D object counter plug-in was used. Statistical analysis was done using Prism5. Statistical significance was analyzed by Mann-Whitney test for the lymph gland phenotypes and one-way ANOVA, for qRT-PCR. Given natural variations in the blood phenotype, we consider $p < 0.01$ as significant. Specific genotypes and raw data are indicated in Supplementary Table S1.

## RESULTS

### Feeding BPS induces crystal cell differentiation in the lymph gland

To understand the importance of iron levels in blood differentiation, we reared larvae on food containing additional iron, ferric ammonium citrate (FAC) or on food containing an iron chelator, bathophenanthroline disulfate (BPS). In normal growing conditions, the lymph gland expresses about 50 crystal cells on average at 25℃ (Fig. 1C). Interestingly, feeding 100 μM BPS significantly increases the number of crystal cells while differentiation of plasmatocytes remains unchanged (Fig. 1C). Supplementation of food with 200 μM BPS delays larval growth and reduces size of the lymph gland, which contributes to the decreased number of crystal cells (Fig. 1C). Differentiation of plasmatocytes or crystal cells is not altered by feeding FAC-supplemented food (Fig. 1D). Changes in iron concentrations by supplementing FAC or BPS were confirmed by performing Prussian blue staining in the intestine. Supplementation of FAC enhances Prussian blue staining in the intestine iron region, while feeding BPS reduces the color (Figs. 1E and 1F). In accordance with this, previous study has shown that dietary supplementation of FAC or BPS desirably alters whole-body iron contents (Tang and Zhou, 2013). Collectively, these data suggest that decreased iron levels during larval development disrupts differentiation of blood cells and increases the number of crystal cells in the lymph gland.

### Loss of *Fer1HCH* in the intestine activates crystal cell differentiation

We next investigated whether alterations in iron homeostasis in the intestine give rise to a similar blood phenotype. To address this, we conducted a mini-screen by knocking-down genes involved in iron regulation including *Mvl*, *mfrn*, *IRP-1A*, *IRP-1B*, *Fer1HCH*, *Fer2LCH*, *Tsf1* and *Tsf3* in the intestine with the use of intestine-specific Gal4, *NP1-gal4* (Cronin et al., 2009), and analyzed blood phenotypes in the lymph gland (Figs. 2A and 2B). Expression of RNAi against *Fer1HCH* significantly induces the differentiation of crystal cells, similar to the phenotype derived by supplementation of BPS (Fig. 2B). However, this genetic background does not modify differentiation of plasmatocytes that are Pxn-positive (Fig. 2C). Knock-down of *Fer1HCH* in the midgut including iron specific region using *Mvl-gal4* reproduces this phenotype (Fig. 2D). Except for *Fer1HCH*, none of the candidate genes causes abnormal blood differentiation in the lymph gland (Fig. 2B). These data suggest that disruption of iron levels induced by expression of *Fer1HCH* RNAi in the midgut generates the disproportionate number of crystal cells.

### Fer1HCH is expressed in the blood

*Drosophila* Fer1HCH is one of the major ferritin complex that associates with Fer2LCH and is known to be expressed in various tissues from embryo to adults (Gonzalez-Morales et al., 2015). Although expressions of both subunits of ferritins are predominant in tissues including the intestine, ferritins are also one of the most abundant proteins isolated in the hemolymph (Georgieva et al., 2002; Handke et al., 2013).

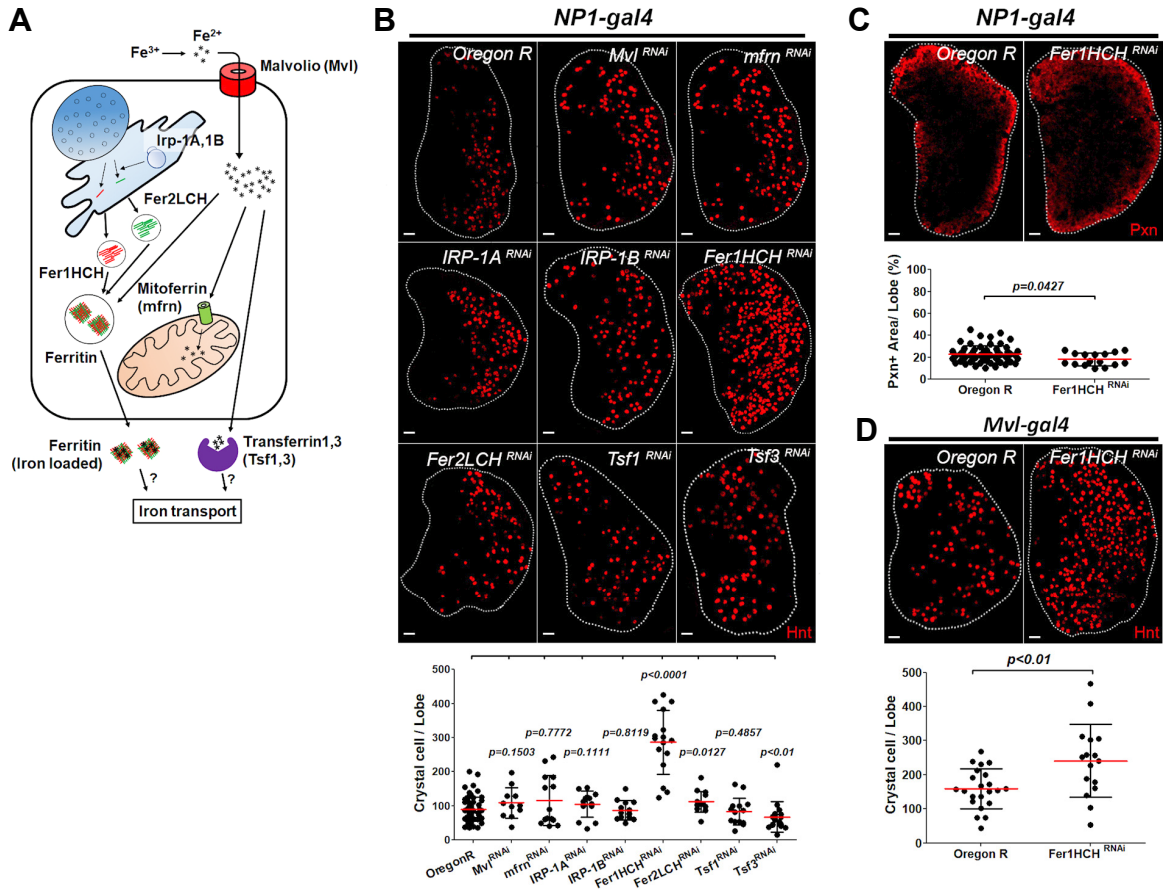


**Fig. 2. Loss of Fer1HCH in the midgut enhances differentiation of crystal cells in the lymph gland.** (A) Schematic representation of *Drosophila* iron control. *Mvl* is a mammalian DMT1/NRAMP2 orthologue that is involved in gut iron absorption. *IRP-1A* and *IRP-1B* are iron-regulatory proteins that bind to iron-responsive elements in mRNAs of iron-related genes. *mfrn* encodes a mitochondrial iron importer. *Fer1HCH* and *Fer2LCH* are subunits for the major iron storage complex. *Tsf1* and *Tsf3* are expected to transport irons to serum. (B) Intestine-specific RNAi of iron homeostasis-related genes revealed that loss of *Fer1HCH* gives rise to excessive crystal cell differentiation. With the use of *NP1-gal4*, eight genes involved in iron control were down-regulated. Loss of *Fer1HCH* activates crystal cell differentiation in the lymph gland (*NP1-gal4 UAS-Fer1HCH*$^{RNAi}$) while other candidate genes do not result in any phenotype (Hnt, red). Quantitation of the mini-screen is shown in the graph. This experiment was done at 29℃ and therefore, one lymph gland lobe exhibits 100 crystal cells on average in controls. (C) Loss of *Fer1HCH* in the intestine does not alter the plasmatocyte differentiation. Expression of Pxn+ plasmatocytes in *Fer1HCH* RNAi (*NP1-gal4 UAS-Fer1HCH*$^{RNAi}$) is comparable to the wild type (Pxn, red). Quantitation of Pxn+ area per lymph gland lobe is indicated in the graph. (D) Midgut-specific RNAi against *Fer1HCH* increases the number of crystal cells in the lymph gland. Midgut iron region-specific expression of *Fer1HCH* RNAi using *Mvl*$^{NP2375}$*-gal4* (*Mvl*$^{NP2375}$*-gal4 UAS-Fer1HCH*$^{RNAi}$) causes identical crystal cell phenotype derived by *NP1-gal4*. Quantitation of the crystal cell expression per lymph gland lobe is shown in the graph. Lymph glands are demarcated by white dotted lines. *p* values are indicated in the graphs. Error bars in the graph represent standard deviation. Scale bar, 20 μm.

To assess detailed expression patterns of *Fer1HCH* in the blood during larval stages, we analyzed expressions of GFP-ferritin trap line, *Fer1HCH*$^{G188}$ (Missirlis et al., 2007). At the wandering third instar, the brain hemispheres except for optic lobes, the ventral nerve cord, the fat body, pericardial cells, Garland cells, intestine and Malpighian tubules express *Fer1HCH*$^{G188}$ in normal growing conditions (Figs. 3A-3B). Interestingly, GFP expression of *Fer1HCH*$^{G188}$ is also found in the lymph gland blood cells (Fig. 3B). *Fer1HCH*$^{G188}$ expression is not restricted to any zone of the lymph gland but shows a sporadic pattern in the entire organ (Fig. 3B). There are two types of expression patterns: few cells exhibit high levels of GFP in the cytosol whereas low GFP$^{+}$ puncta are seen throughout the lymph gland regardless of the zone, similar to the pattern observed in the intestine (Missirlis et al., 2007) (Fig. 3B). These puncta are not Rab5 positive, indicating that Fer1HCH protein is not a part of the endocytic pathway (Fig. 3B). To analyze expression patterns of *Fer1HCH*$^{G188}$ in the lymph gland in detail, we co-stained *Fer1HCH*$^{G188}$ with Dome, Pxn or Hnt. Few *Fer1HCH*$^{G188}$-GFP are expressed in Dome$^{+}$ progenitor cells, but not all lymph gland exhibits Dome$^{+}$ *Fer1HCH*$^{G188}$-GFP$^{+}$ blood cells (Fig. 3B).

This is also true for crystal cells: some Hnt$^{+}$ crystal cells express low *Fer1HCH*$^{G188}$-GFP while majority of crystal cells do not show *Fer1HCH*$^{G188}$-GFP. Nearly all Pxn$^{+}$ mature blood cells display either high or low *Fer1HCH*$^{G188}$*-GFP* expression (Fig. 3B). Circulating blood cells also exhibit *Fer1HCH*$^{G188}$ expression, again, most of which are co-stained with Pxn (Fig. 3C).

Expression of ferritin in the intestine is a consequence of an iron availability. Feeding FAC supplemented food raises *Fer1HCH*$^{G188}$ expressions as well as Fer1HCH protein levels in the intestine (Missirlis et al., 2007). Yet, it is unclear whether *Fer1HCH*$^{G188}$ in the lymph gland reacts to different levels of systemic iron as in the intestine. We found that supplementation of 5 mM FAC upregulates *Fer1HCH*$^{G188}$ GFP in the lymph gland while feeding 100 μM BPS does not alter the expression (Fig. 3D). Moreover, endogenous expression of *Fer1HCH* in the blood is verified by qRT-PCR which showed that *Fer1HCH* RNAi in the blood dramatically reduces normal mRNA levels of *Fer1HCH* (Fig. 3E). Taken together, our findings indicate that *Fer1HCH* is expressed in the blood population in addition to previously identified organs and readily responds to systemic iron concentrations.

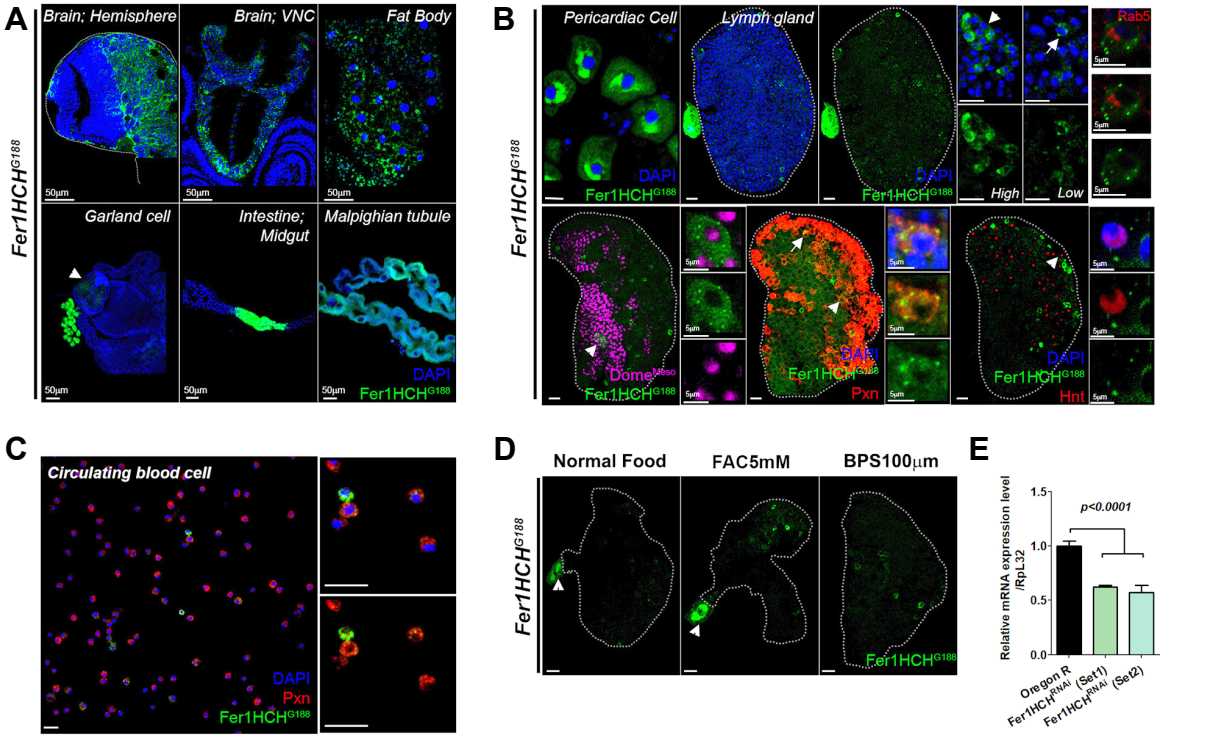


**Fig. 3. Fer1HCH is expressed in the blood.** (A) Expression of GFP-tagged trap line, *Fer1HCH*$^{G188}$ in larval organs. (Top) *Fer1HCH*$^{G188}$ is expressed in the brain hemispheres, the ventral nerve cord, the fat body, (Bottom) Garland cells, midgut iron region and Malphigian tubule. Garland cells are adjacent to the foregut (arrowhead) and iron region is in the middle of the intestine (Fer1HCH-GFP, green; DAPI, blue). (B) *Fer1HCH*$^{G188}$ is expressed in the lymph gland. (Top) Pericardial cells express high levels of *Fer1HCH-GFP*. Lymph gland exhibits a sporadic pattern of *Fer1HCH*$^{G188}$*-GFP*. Two distinctive expressions are observed. Cytosolic high *Fer1HCH*$^{G188}$*-GFP* is seen in the lymph gland blood cells (arrowhead). Punctated low *Fer1HCH*$^{G188}$*-GFP* is expressed throughout the lymph gland (arrow). Rab5 is not co-localized with *Fer1HCH*$^{G188}$*-GFP* expressing puncta (Fer1HCH-GFP, green; Rab5, red; DAPI, blue). (Bottom) A subset of Dome+ cells express *Fer1HCH*$^{G188}$*-GFP* (arrowhead). Not all lymph gland displays Dome$^{+}$Fer1HCH$^{+}$ expression. However, if found, Dome$^{+}$Fer1HCH$^{+}$ cells compose a cluster in the MZ (Dome, magenta; Fer1HCH-GFP, green). Pxn$^{+}$ cells are co-localized with either high (arrow) or low (arrowhead) *Fer1HCH*$^{G188}$*-GFP* (Pxn, red; Fer1HCH-GFP, green; DAPI, blue). Few Hnt$^{+}$ crystal cells express low *Fer1HCH*$^{G188}$*-GFP* (arrowhead; Hnt, red; Fer1HCH-GFP, green; DAPI, blue). High magnification images of each samples are indicated in insets. (C) *Fer1HCH*$^{G188}$*-GFP* is expressed in circulating blood cells. Similar to the lymph gland, there is a mixture of high and low *Fer1HCH*$^{G188}$*-GFP* in the circulating blood. *Fer1HCH*$^{G188}$*-GFP* positive cells in circulation are Pxn$^{+}$. Both high and low *Fer1HCH*$^{G188}$*-GFP* positive cells are co-localized with Pxn (Pxn, red; Fer1HCH-GFP, green; DAPI, blue). High magnification images are indicated in insets.(D) *Fer1HCH*$^{G188}$*-GFP* in the lymph gland responds to higher levels of systemic iron. Feeding 5 mM FAC induces *Fer1HCH*$^{G188}$*-GFP* expression in the lymph gland. However, 100 μM BPS-mediated chelation of iron does not alter the expression (Fer1HCH-GFP, green). Images are middle three stacks of the lymph gland. Arrowhead indicates the pericardial cell. (E) Expression of *Fer1HCH* RNAi with the use of *Hml-gal4* (*Hml-gal4 UAS-Fer1HCH*$^{RNAi}$) reduces the relative expression of *Fer1HCH* mRNA levels. Set 1 and Set 2 indicate different sets of primers used in qRT-PCR. Sequences of primers are shown in methods. Lymph glands are demarcated by white dotted lines. *p* values are indicated in the graphs. Error bars in the graph represent standard deviation. Scale bar, 20 μm unless otherwise indicated.

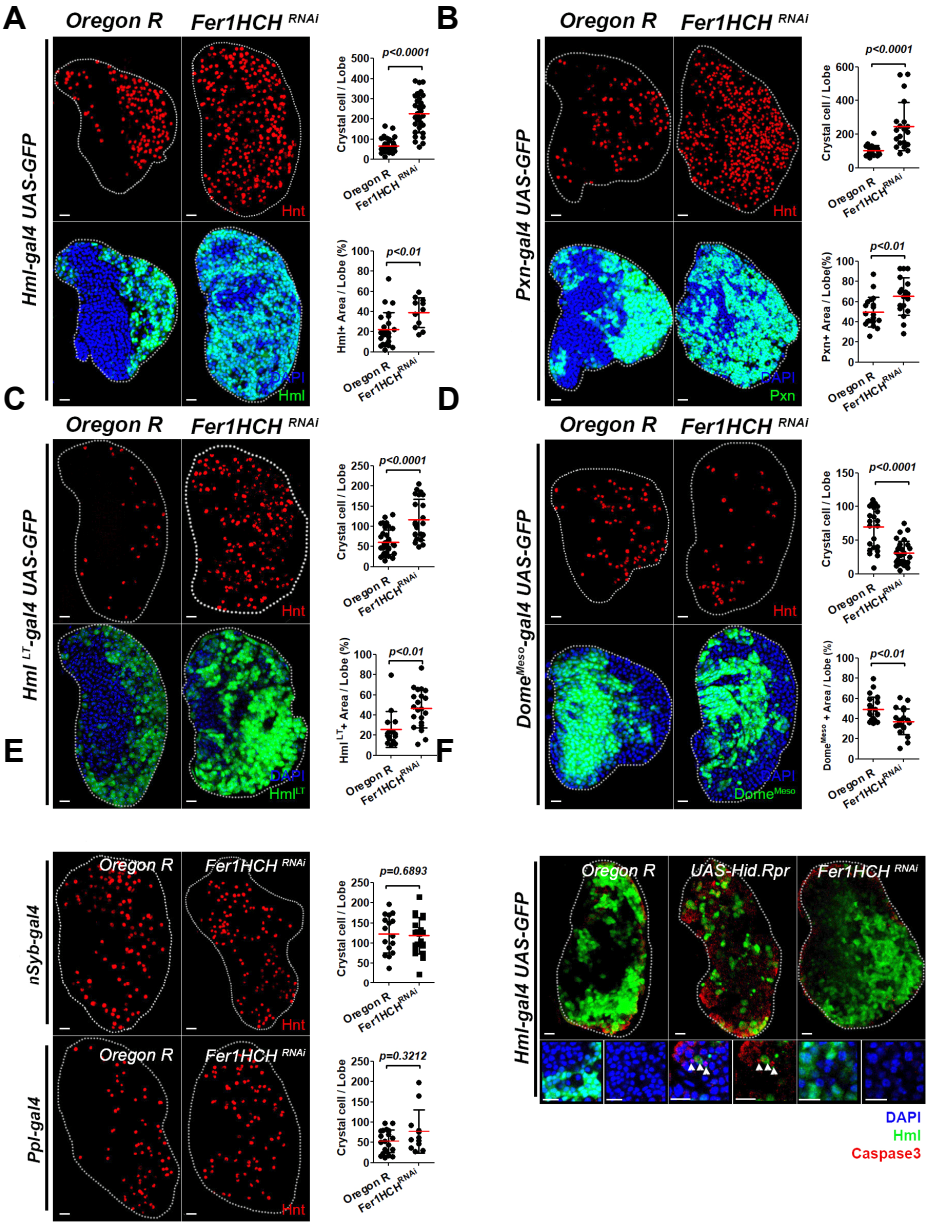


**Fig. 4. Loss of *Fer1HCH* in blood cells causes abnormal differentiation of the lymph gland.** (A) *Fer1HCH* RNAi in mature blood cells, particularly plasmatocytes, causes expansion of the CZ. (Top) Loss of *Fer1HCH* in mature blood cells (*Hml-gal4 UAS-Fer1HCH*$^{RNAi}$) increases the number of crystal cells (Hnt, red). Graph indicates quantitation of the number of Hnt+ crystal cells per lymph gland lobe. (Bottom) RNAi against *Fer1HCH* in mature blood cells (*Hml-gal4 UAS-Fer1HCH*$^{RNAi}$) reduces the MZ and shows an increase in the CZ (Hml, green; DAPI, blue). Graph indicates quantitation of Hml+ mature blood cells per lymph gland lobe. (B) Expression of RNAi against *Fer1HCH* in plasmatocytes leads to exacerbated CZ differentiation. (Top) Loss of *Fer1HCH* in the CZ (*Pxn-gal4 UAS-Fer1HCH*$^{RNAi}$) increases the number of crystal cells (Hnt, red). Graph indicates quantitation of the number of Hnt+ crystal cells per lymph gland lobe. (Bottom) *Fer1HCH* RNAi in mature blood cells (*Pxn-gal4 UAS-Fer1HCH*$^{RNAi}$) decreases the MZ and expands the CZ (Pxn, green; DAPI, blue). Graph indicates quantitation of Pxn+ mature blood cells per lymph gland lobe. (C) Knock-down of *Fer1HCH* in mature blood cells including both plasmatocytes and crystal cells results in excessive differentiation of the CZ. (Top) Loss of *Fer1HCH* in the mature blood cells (*Hml$^{LT}$-gal4 UAS-Fer1HCH*$^{RNAi}$) activates crystal cell differentiation (Hnt, red). Graph indicates quantitation of the number of Hnt+ crystal cells per lymph gland lobe. (Bottom) RNAi against *Fer1HCH* in mature blood cells (*Hml$^{LT}$-gal4 UAS-Fer1HCH*$^{RNAi}$) diminishes the MZ and expands the CZ (Hml, green; DAPI, blue). Graph indicates quantitation of Hml$^{LT}$+ mature blood cells per lymph gland lobe. (D) RNAi against *Fer1HCH* in blood progenitors results in reduced differentiation of crystal cells. (Top) Loss of *Fer1HCH* in the MZ (*Dome$^{Meso}$-gal4 UAS-Fer1HCH*$^{RNAi}$) suppresses crystal cell differentiation (Hnt, red). Graph indicates quantitation of the number of Hnt+ crystal cells per lymph gland lobe. (Bottom) Expression of *Fer1HCH* RNAi in blood progenitors (*Dome$^{Meso}$-gal4 UAS-Fer1HCH*$^{RNAi}$) leads to moderate decrease in the MZ (*Dome$^{Meso}$*, green; DAPI, blue). Graph indicates quantitation of *Dome$^{Meso}$* + blood progenitor cells per lymph gland lobe. (E) Loss of *Fer1HCH* in neurons or in the fat body does not alter the number of crystal cells. (Top) Neuron-specific *nSyb-gal4* driving *Fer1HCH* RNAi (*nSyb-gal4 UAS-Fer1HCH*$^{RNAi}$) does not change the number of crystal cells in the lymph gland (Hnt, red). Quantitation of crystal cell differentiation is indicated in the graph. (Bottom) Fat body-specific *Ppl-gal4* driving *Fer1HCH* RNAi (*Ppl-gal4 UAS-Fer1HCH*$^{RNAi}$) does not modify differentiation of crystal cells (Hnt, red). Quantitation of crystal cell numbers is shown in the graph. (F) Lymph glands with *Fer1HCH* RNAi in mature blood cells do not induce cell death. Expression of pro-apoptotic genes, *Hid* and *Rpr* in the CZ (*Hml-gal4 UAS-Hid, Rpr*) enhances active Caspase3 expression in the lymph gland. Magnified view in insets. Arrowhead indicates active Caspase3-positive puncta in Hml+ blood cells. This expression is not seen when *Fer1HCH* RNAi is expressed in the CZ (*Hml-gal4 UAS-Fer1HCH*$^{RNAi}$) (Hml, green; active Caspase3, red; DAPI, blue). Lymph glands are demarcated by white dotted lines. *p* values are indicated in the graphs. Error bars in the graph represent standard deviation. Scale bar, 20 μm.

### Fer1HCH plays a key role in blood development

Novel function of *Fer1HCH* in the blood is further assessed by knocking-down its expression in the lymph gland. Based on its sporadic pattern in the lymph gland, we analyzed functions of *Fer1HCH* in each zone by expressing RNAi against *Fer1HCH* with zone-specific drivers. Mature blood cell-specific knock-down of *Fer1HCH* using *Hml-gal4* or *Pxn-gal4* leads to a dramatic increase in the number of crystal cells when compared to wild types (Figs. 4A and 4B). Different from the intestine-specific knock-down, these genetic backgrounds also aggravate plasmatocyte differentiation and cause a marked increase of the CZ (Figs. 4A and 4B). These phenotypes are recapitulated by expressing RNAi against *Fer1HCH* in $Hml^{+}$ lineage-traced population using *Hml-gal4* lineage traced line (Fig. 4C). However, crystal cell differentiation is reduced by knocking-down the expression of *Fer1HCH* in progenitor blood cells with the use of *Dome-Meso-gal4* (Fig. 4D). Brain-specific knock-down or fat body-specific RNAi against *Fer1HCH* does not impinge on blood development in the lymph gland (Fig. 4E).

Previous studies indicated that expression of pro-apoptotic genes, *Hid* and *Rpr* in the CZ causes loss of blood progenitors and subsequent differentiation of mature blood cells (Mondal et al., 2011). Similar phenotype is observed when $Fer1HCH^{RNAi}$ is expressed in mature blood cells (Figs. 4A-4C). We reasoned that this phenotype generated by $Fer1HCH^{RNAi}$ is due to programmed cell death. However, *Fer1HCH* RNAi in mature blood cells do not accumulate Caspase3 expression in the lymph gland (Fig. 4F), implying that inordinate expansion of the CZ is not a consequence of regular cell death. Thus, these findings establish that Fer1HCH in the blood maintains iron homeostasis and loss of iron control gives rise to abnormal blood cell differentiation mimicking stress responses.

## DISCUSSION

This research identified iron homeostasis as one of the key factors that govern blood differentiation of *Drosophila* larva through expressions of ferritins in the intestine and the blood. Feeding 100 μM BPS is sufficient to cause extensive differentiation of the crystal cell in the lymph gland without altering larval development. BPS-mediated blood response is repeated when *Fer1HCH* RNAi is expressed in the intestine iron region while RNAi against other iron-related genes does not modify the crystal cell number. Consistent with these findings, previous study has shown that expression of RNAi against *Fer1HCH* in the intestine suppresses whole-body iron levels (Tang and Zhou, 2013). This indicates that both dietary BPS and *Fer1HCH* RNAi diminishes systemic iron levels leading to the abnormal crystal cell differentiation. Crystal cells exhibit expression of Prophenoloxidase (ProPO) essential for activation of melanization and immune responses (Rizki et al., 1985). Therefore, understanding physiological roles of crystal cells in iron-mediated immunity will be interesting.

*Fer1HCH* interacts with *Fer2LCH* in the generation of iron-storage cluster (Mandilaras et al., 2013) and expression of these genes are strictly regulated by iron levels through IRPs (Georgieva et al., 1999). However, we could not detect any blood phenotype by inhibiting *Fer2LCH* in the intestine. Similarly, recent study has shown that loss of *Fer2HCH* in the intestine does not suppress the whole-body iron levels (Tang and Zhou, 2013). In the brain, *Fer1HCH* RNAi in specific neurons do not alter the circadian rhythms while *Fer2LCH* does (Mandilaras and Missirlis, 2012). These notions together imply that *Fer1HCH* and *Fer2LCH* could take part in distinctive pathways in addition to the core function of iron storage.

Iron sequestration is a critical response in innate immunity as acquisition of iron is an important element for pathogenic proliferation (Drakesmith and Prentice, 2012). In *Drosophila*, expressions of iron regulatory proteins are increased upon bacterial or fungal infections (Sulieman et al., 2004; Yoshiga et al., 1999). A similar response is observed when flies are infected by *Wolbachia* (Brownlie et al., 2009; Kremer et al., 2009). Our results identified a novel role for iron in blood development that is closely related to the innate immune reaction. As mentioned above, crystal cells react to iron chelation. However, it is unclear how the whole-body iron levels are connected to the differentiation of crystal cells. It is possible that loss of iron directly affects signaling pathways including Serrate-Notch or Lozenge, or modifies unknown systemic factors that merge onto the crystal cell differentiation mechanism.

Our study first demonstrates that functional ferritin is expressed in the lymph gland and loss of *Fer1HCH* leads to abnormal blood phenotypes. Although *Fer1HCH* RNAi in the blood or intestine alters blood development, these two phenotypes are not precisely identical. Loss of *Fer1HCH* in the intestine only gives rise to excessive crystal cells in the lymph gland without disrupting the ratio of the CZ. *Fer1HCH* RNAi in the CZ promotes differentiation of both crystal cells and plasmatocytes and consequently reduces the MZ. When *Fer1HCH* is knocked-down in the MZ, moderate decrease in the MZ ratio and the number of crystal cells are observed. These phenotypes suggest that *Fer1HCH* in the blood may play different roles in each zone. It is interesting to note that *Fer1HCH* RNAi in the blood substantially increases the CZ without enhancing active Caspase3 expression, implying an alternative pathway that aggravates the CZ via the function of Fer1HCH. Recent studies have shown that loss of *Fer1HCH* elevates cellular iron concentration leading to ferroptosis in larval discs. This phenomenon is separable from apoptosis, necrosis or autophagy (Dixon and Stockwell, 2014; Dixon et al., 2012; Tang and Zhou, 2013). Ferroptosis is reported recently in mammalian cancer cells and fibroblasts (Dixon and Stockwell, 2014). Precise roles and detailed mechanisms underlying this phenomenon is unclear. *Drosophila* blood system will be a useful tool to uncover mechanistic details and for identification of novel factors involved in ferroptosis.

Ferritins in the midgut iron region are responsible for the control of systemic iron levels (Tang and Zhou, 2013). However, it is uncertain whether ferritins expressed in other tissues are equally accountable to the iron homeostasis. Different from mammals, significant amounts of ferritin proteins are deposited into the circulation of *Drosophila* (Handke et al., 2013). However, origins of these circulating ferritins are

still elusive. Surprisingly, we observed that larvae expressing *Fer1HCH* RNAi in the blood experience growth retardation when fed BPS (data not shown). This observation implies a considerable contribution of blood ferritins in the systemic iron homeostasis eliciting future studies on the role of blood in iron regulation. Thus, our study uncovers iron homeostasis as a crucial player in blood development, and suggests an interesting possibility that ferritin in the blood may take part in the systemic iron control.

*Note: Supplementary information is available on the Molecules and Cells website (www.molcells.org).*

## ACKNOWLEDGMENTS

We thank Hyejin Lee for *Hml$^{\Delta}$-gal4* analysis. We acknowledge the Bloomington, VDRC and DGRC *Drosophila* stock centers and the DSHB hybridoma bank. We thank the following individuals for stocks and reagents: U. Banerjee, J. Fessler and S. Sinenko. This work was supported by the National Research Foundation (NRF) grant funded by the Korean government (NRF-2017R1C1B2007343) and the research fund of Hanyang University (HY-2014-N) to J.S.

## REFERENCES

Agaisse, H., and Perrimon, N. (2004). The roles of JAK/STAT signaling in Drosophila immune responses. Immunol. Rev. *198*, 72-82.

Benmimoun, B., Polesello, C., Waltzer, L., and Haenlin, M. (2012). Dual role for Insulin/TOR signaling in the control of hematopoietic progenitor maintenance in Drosophila. Development *139*, 1713-1717.

Brownlie, J.C., Cass, B.N., Riegler, M., Witsenburg, J.J., Iturbe-Ormaetxe, I., McGraw, E.A., and O'Neill, S.L. (2009). Evidence for metabolic provisioning by a common invertebrate endosymbiont, Wolbachia pipientis, during periods of nutritional stress. PLoS Pathog. *5*, e1000368.

Cronin, S.J., Nehme, N.T., Limmer, S., Liegeois, S., Pospisilik, J.A., Schramek, D., Leibbrandt, A., Simoes Rde, M., Gruber, S., Puc, U., et al. (2009). Genome-wide RNAi screen identifies genes involved in intestinal pathogenic bacterial infection. Science *325*, 340-343.

De Domenico, I., McVey Ward, D., and Kaplan, J. (2008). Regulation of iron acquisition and storage: consequences for iron-linked disorders. Nat. Rev. Mol. Cell Biol. *9*, 72-81.

Dixon, S.J., Lemberg, K.M., Lamprecht, M.R., Skouta, R., Zaitsev, E.M., Gleason, C.E., Patel, D.N., Bauer, A.J., Cantley, A.M., Yang, W.S., et al. (2012). Ferroptosis: an iron-dependent form of nonapoptotic cell death. Cell *149*, 1060-1072.

Dixon, S.J., and Stockwell, B.R. (2014). The role of iron and reactive oxygen species in cell death. Nat. Chem. Biol. *10*, 9-17.

Dragojlovic-Munther, M., and Martinez-Agosto, J.A. (2012). Multifaceted roles of PTEN and TSC orchestrate growth and differentiation of Drosophila blood progenitors. Development *139*, 3752-3763.

Drakesmith, H., and Prentice, A.M. (2012). Hepcidin and the iron-infection axis. Science *338*, 768-772.

Evans, C.J., Hartenstein, V., and Banerjee, U. (2003). Thicker than blood: conserved mechanisms in Drosophila and vertebrate hematopoiesis. Dev. Cell *5*, 673-690.

Georgieva, T., Dunkov, B.C., Harizanova, N., Ralchev, K., and Law, J.H. (1999). Iron availability dramatically alters the distribution of ferritin subunit messages in Drosophila melanogaster. Proc. Natl. Acad. Sci. USA *96*, 2716-2721.

Georgieva, T., Dunkov, B.C., Dimov, S., Ralchev, K., and Law, J.H. (2002). Drosophila melanogaster ferritin: cDNA encoding a light chain homologue, temporal and tissue specific expression of both subunit types. Insect. Biochem. Mol. Biol. *32*, 295-302.

Gold, K.S., and Bruckner, K. (2015). Macrophages and cellular immunity in Drosophila melanogaster. Semin. Immunol. *27*, 357-368.

Gonzalez-Morales, N., Mendoza-Ortiz, M.A., Blowes, L.M., Missirlis, F., and Riesgo-Escovar, J.R. (2015). Ferritin Is Required in Multiple Tissues during Drosophila melanogaster Development. PLoS One *10*, e0133499.

Grigorian, M., Mandal, L., and Hartenstein, V. (2011). Hematopoiesis at the onset of metamorphosis: terminal differentiation and dissociation of the Drosophila lymph gland. Dev. Genes Evol. *221*, 121-131.

Handke, B., Poernbacher, I., Goetze, S., Ahrens, C.H., Omasits, U., Marty, F., Simigdala, N., Meyer, I., Wollscheid, B., Brunner, E., et al. (2013). The hemolymph proteome of fed and starved Drosophila larvae. PLoS One *8*, e67208.

Jung, S.H., Evans, C.J., Uemura, C., and Banerjee, U. (2005). The Drosophila lymph gland as a developmental model of hematopoiesis. Development *132*, 2521-2533.

Khadilkar, R.J., Ray, A., Chetan, D.R., Sinha, A.R., Magadi, S.S., Kulkarni, V., and Inamdar, M.S. (2017). Differential modulation of the cellular and humoral immune responses in Drosophila is mediated by the endosomal ARF1-Asrij axis. Sci. Rep. *7*, 118.

Kremer, N., Voronin, D., Charif, D., Mavingui, P., Mollereau, B., and Vavre, F. (2009). Wolbachia interferes with ferritin expression and iron metabolism in insects. PLoS Pathog. *5*, e1000630.

Lanot, R., Zachary, D., Holder, F., and Meister, M. (2001). Postembryonic hematopoiesis in Drosophila. Dev. Biol. *230*, 243-257.

Lebestky, T., Jung, S.H., and Banerjee, U. (2003). A Serrate-expressing signaling center controls Drosophila hematopoiesis. Genes Dev. *17*, 348-353.

Letourneau, M., Lapraz, F., Sharma, A., Vanzo, N., Waltzer, L., and Crozatier, M. (2016). Drosophila hematopoiesis under normal conditions and in response to immune stress. FEBS Lett. *590*, 4034-4051.

Mandal, L., Martinez-Agosto, J.A., Evans, C.J., Hartenstein, V., and Banerjee, U. (2007). A Hedgehog- and Antennapedia-dependent niche maintains Drosophila haematopoietic precursors. Nature *446*, 320-324.

Mandilaras, K., and Missirlis, F. (2012). Genes for iron metabolism influence circadian rhythms in Drosophila melanogaster. Metallomics *4*, 928-936.

Mandilaras, K., Pathmanathan, T., and Missirlis, F. (2013). Iron absorption in Drosophila melanogaster. Nutrients *5*, 1622-1647.

Missirlis, F., Holmberg, S., Georgieva, T., Dunkov, B.C., Rouault, T.A., and Law, J.H. (2006). Characterization of mitochondrial ferritin in Drosophila. Proc. Natl. Acad. Sci. USA *103*, 5893-5898.

Missirlis, F., Kosmidis, S., Brody, T., Mavrakis, M., Holmberg, S., Odenwald, W.F., Skoulakis, E.M., and Rouault, T.A. (2007). Homeostatic mechanisms for iron storage revealed by genetic manipulations and live imaging of Drosophila ferritin. Genetics *177*, 89-100.

Mondal, B.C., Mukherjee, T., Mandal, L., Evans, C.J., Sinenko, S.A., Martinez-Agosto, J.A., and Banerjee, U. (2011). Interaction between differentiating cell- and niche-derived signals in hematopoietic progenitor maintenance. Cell *147*, 1589-1600.

Morin-Poulard, I., Vincent, A., and Crozatier, M. (2013). The Drosophila JAK-STAT pathway in blood cell formation and immunity. JAKSTAT *2*, e25700.

Mukherjee, T., Kim, W.S., Mandal, L., and Banerjee, U. (2011). Interaction between Notch and Hif-alpha in development and survival of Drosophila blood cells. Science *332*, 1210-1213.

Owusu-Ansah, E., and Banerjee, U. (2009). Reactive oxygen species prime Drosophila haematopoietic progenitors for differentiation. Nature *461*, 537-541.

Ponka, P. (1997). Tissue-specific regulation of iron metabolism and heme synthesis: distinct control mechanisms in erythroid cells. Blood *89*, 1-25.

Qiu, P., Pan, P.C., and Govind, S. (1998). A role for the Drosophila Toll/Cactus pathway in larval hematopoiesis. Development *125*, 1909-1920.

Rizki, T.M., and Rizki, R.M. (1978). Larval adipose tissue of homoeotic bithorax mutants of Drosophila. Dev. Biol. *65*, 476-482.

Rizki, T.M., Rizki, R.M., and Bellotti, R.A. (1985). Genetics of a Drosophila phenoloxidase. Mol. Gen. Genet. *201*, 7-13.

Rouault, T.A., and Tong, W.H. (2005). Iron-sulphur cluster biogenesis and mitochondrial iron homeostasis. Nat. Rev. Mol. Cell Biol. *6*, 345-351.

Santambrogio, P., Levi, S., Cozzi, A., Corsi, B., and Arosio, P. (1996). Evidence that the specificity of iron incorporation into homopolymers of human ferritin L- and H-chains is conferred by the nucleation and ferroxidase centres. Biochem. J. *314 ( Pt 1)*, 139-144.

Sheftel, A.D., Mason, A.B., and Ponka, P. (2012). The long history of iron in the Universe and in health and disease. Biochim. Biophys. Acta *1820*, 161-187.

Shim, J. (2015). Drosophila blood as a model system for stress sensing mechanisms. BMB Rep *48*, 223-228.

Shim, J., Mukherjee, T., and Banerjee, U. (2012). Direct sensing of systemic and nutritional signals by haematopoietic progenitors in Drosophila. Nat. Cell Biol. *14*, 394-400.

Shim, J., Gururaja-Rao, S., and Banerjee, U. (2013). Nutritional regulation of stem and progenitor cells in Drosophila. Development *140*, 4647-4656.

Sinenko, S.A., Shim, J., and Banerjee, U. (2011). Oxidative stress in the haematopoietic niche regulates the cellular immune response in Drosophila. EMBO Rep. *13*, 83-89.

Sorrentino, R.P., Carton, Y., and Govind, S. (2002). Cellular immune response to parasite infection in the Drosophila lymph gland is developmentally regulated. Dev. Biol. *243*, 65-80.

Sulieman, M., Asleh, R., Cabantchik, Z.I., Breuer, W., Aronson, D., Suleiman, A., Miller-Lotan, R., Hammerman, H., and Levy, A.P. (2004). Serum chelatable redox-active iron is an independent predictor of mortality after myocardial infarction in individuals with diabetes. Diabetes Care *27*, 2730-2732.

Tang, X., and Zhou, B. (2013). Ferritin is the key to dietary iron absorption and tissue iron detoxification in Drosophila melanogaster. FASEB J. *27*, 288-298.

Waltzer, L., Gobert, V., Osman, D., and Haenlin, M. (2010). Transcription factor interplay during Drosophila haematopoiesis. Int. J. Dev. Biol. *54*, 1107-1115.

Yoshiga, T., Georgieva, T., Dunkov, B.C., Harizanova, N., Ralchev, K., and Law, J.H. (1999). Drosophila melanogaster transferrin. Cloning, deduced protein sequence, expression during the life cycle, gene localization and up-regulation on bacterial infection. Eur. J. Biochem. *260*, 414-420.

Zettervall, C.J., Anderl, I., Williams, M.J., Palmer, R., Kurucz, E., Ando, I., and Hultmark, D. (2004). A directed screen for genes involved in Drosophila blood cell activation. Proc. Natl. Acad. Sci. USA *101*, 14192-14197.